Journal of Cellular Physiology

HhAntag, a Hedgehog Signaling Antagonist, Suppresses Chondrogenesis and Modulates Canonical and Non-Canonical BMP Signaling

CHRISTINA MUNDY,[1]* ADEBAYO BELLO,[2] FEDERICA SGARIGLIA,[1] EIKI KOYAMA,[1] AND MAURIZIO PACIFICI[1]

[1]*Translational Research Program in Pediatric Orthopaedics, Division of Orthopaedic Surgery, The Children's Hospital of Philadelphia, Philadelphia, Pennsylvania*

[2]*Bucknell University, Lewisburg, Pennsylvania*

Chondrogenesis subtends the development of most skeletal elements and involves mesenchymal cell condensations differentiating into growth plate chondrocytes that proliferate, undergo hypertrophy, and are replaced by bone. In the pediatric disorder Hereditary Multiple Exostoses, however, chondrogenesis occurs also at ectopic sites and causes formation of benign cartilaginous tumors—exostoses—near the growth plates. No treatment is currently available to prevent or reverse exostosis formation. Here, we asked whether chondrogenesis could be stopped by targeting the hedgehog pathway, one of its major regulators. Micromass cultures of limb mesenchymal cells were treated with increasing amounts of the hedgehog inhibitor HhAntag or vehicle. The drug effectively blocked chondrogenesis and did so in a dose-dependent manner as monitored by: alcian blue-positive cartilage nodule formation; gene expression of cartilage marker genes; and reporter activity in *Gli1-LacZ* cell cultures. HhAntag blocked chondrogenesis even when the cultures were co-treated with bone morphogenetic protein 2 (rhBMP-2), a strong pro-chondrogenic factor. Immunoblots showed that HhAntag action included modulation of canonical (pSmad1/5/8) and non-canonical (pp38) BMP signaling. In cultures co-treated with HhAntag plus rhBMP-2, there was a surprising strong up-regulation of pp38 levels. Implantation of rhBMP-2-coated beads near metacarpal elements in cultured forelimb explants induced formation of ectopic cartilage that however, was counteracted by HhAntag co-treatment. Collectively, our data indicate that HhAntag inhibits not only hedgehog signaling, but also modulates canonical and non-canonical BMP signaling and blocks basal and rhBMP2-stimulated chondrogenesis, thus representing a potentially powerful drug-based strategy to counter ectopic cartilage growth or induce its involution.
J. Cell. Physiol. 231: 1033–1044, 2016. © 2015 Wiley Periodicals, Inc.

The formation of most skeletal elements in the developing embryo initiates with the emergence of mesenchymal and ectomesenchymal cell condensations at prescribed sites and times (Mackie et al., 2011). The condensed cells then undergo cell differentiation into chondrocytes, and the resulting cartilaginous anlagen constitute the blueprint and framework of the future skeleton. The newly-formed chondrocytes reorganize themselves into growth plates that display typical proliferative, prehypertrophic, and hypertrophic zones of maturation, and the hypertrophic mineralized chondrocytes are eventually replaced by endochondral bone, thus eliciting the emergence of definitive bony skeletal elements (Mackie et al., 2011). These essential processes have been studied for years, and much is known about their cellular, biochemical, and molecular regulation (Kronenberg, 2003). Prominent amongst such regulatory mechanisms are protein signaling pathways and in particular the hedgehog and bone morphogenetic protein (BMP) pathways both of which are pro-chondrogenic, while the Wnt signaling pathway is anti-chondrogenic (Lefebvre and Bhattaram, 2010). Under normal circumstances, these various pathways work in concert to establish and promote, but also limit and delimit, the overall patterns of chondrogenesis and skeletal element definition and growth within the limbs, trunk, and portions of the skull (Lefebvre and Bhattaram, 2010).

There are pathological situations, however, where chondrogenesis can go awry and can occur at ectopic and abnormal sites and times within and along the developing and growing skeleton, thus eliciting a variety of cartilaginous tumor phenotypes and other defects (Mundlos and Olsen, 1997). One such pathology is Hereditary Multiple Exostoses (HME), a congenital autosomal-dominant pediatric disorder that is characterized by benign cartilaginous tumors—exostoses—that form along the perichondrial border of growth plates in long bones, pelvis, vertebrae, and ribs (Björnsson et al., 1998). Because of their location, number, and size, the exostoses can, and do, lead to numerous health problems including skeletal deformities, growth retardation, and chronic pain (Björnsson et al., 1998). The majority of HME cases are caused by loss-of-function mutations in the Golgi-associated and heparan sulfate

Conflict of interest: None.

Contract grant sponsor: Maurizio Pacifici and Eiki Koyama;
Contract grant number: R01AR061758.

*Correspondence to: Christina Mundy, Division of Orthopaedic Surgery, The Children's Hospital of Philadelphia, 3615 Civic Center Boulevard, ARC Suite 902, Philadelphia, PA.
E-mail address: matticolac@email.chop.edu

Manuscript Received: 18 May 2015
Manuscript Accepted: 10 September 2015

Accepted manuscript online in Wiley Online Library (wileyonlinelibrary.com): 12 September 2015.
DOI: 10.1002/jcp.25192

© 2015 WILEY PERIODICALS, INC.

(HS)-synthesizing enzymes EXT1 or EXT2, resulting in systemic HS deficiency (Ahn et al., 1995, Lind et al., 1998). The HS chains are components of cell surface- and extracellular matrix-associated proteoglycans. Interestingly, an important role of these macromolecules is to interact with several HS-binding growth factors and signaling proteins including hedgehog proteins and bone morphogenetic proteins (BMPs), and they can thus regulate protein distribution, bioavailability and target of action and in turn chondrogenesis, as pointed out above (Bernfield et al., 1999, Koziel et al., 2004, Lin, 2004, Jiao et al., 2007).

Given the binding potential of these signaling proteins to HS, a deficiency in HS such as that occurring in HME could lead to increased protein bioavailability and range of action, resulting in wider receptor binding and signaling activation and in turn, abnormal and ectopic chondrogenesis. This scenario would be of particular relevance to sites in the growing skeleton where there are abundant chondroprogenitor cells such as the inner layer of perichondrium where exostoses are in fact thought to most likely originate (Porter and Simpson, 1999, Hecht et al., 2005). Indeed, we found that when *Ext1* was conditionally ablated along long bones in transgenic mice, perichondrial cells flanking the epiphyseal growth plates exhibited increased BMP signaling that was followed by ectopic exostosis-like cartilage formation over time (Huegel et al., 2013). We observed a similar stimulation of chondrogenesis and BMP signaling in cell cultures in which HS was inhibited by genetic, enzymatic, or pharmacological means (Huegel et al., 2013). These data suggested that BMP signaling is a pathway likely dysregulated in HME. An additional and possibly equally important pathway is the hedgehog signaling pathway and in particular, signaling elicited by Indian hedgehog (Ihh). Bruce et al., examined the role of hedgehog signaling in the initial stages of condensation and chondrocyte differentiation in a ligand-independent constitutively-active hedgehog signaling mouse model, Prx 1-Cre:Ptc1$^{c/c}$. The in vivo and in vitro findings suggested that although mesenchymal condensation was not affected, differentiation to cartilage was impaired. Several studies support a role for Ihh during endochondral ossification by regulating chondrocyte proliferation and hypertrophy in the growth plate (Vortkamp et al., 1996, Stott and Chuong, 1997, St-Jacques et al., 1999). Futhermore, Ihh promotes chondrocyte differentiation and cartilage formation in vivo and in vitro (Murtaugh et al., 1999, Enomoto-Iwamoto et al., 2000). Collectively, these studies suggest distinct roles of hedgehog signaling during early chondrogenesis and skeletal development. *Ihh* is normally expressed in the prehypertrophic zone of the growth plate, and its signaling action is most obvious and strong within the growth plate itself and to a lesser extent along perichondrium flanking the prehypertrophic zone (Koyama et al., 1996, Vortkamp et al., 1996). Ihh elicits biological action by binding to the cell surface receptor Patched 1 (Ptch1) that induces the activity of the signaling receptor Smoothened (Smo), activation of Gli transcription factors and modulation of target gene expression. Hedgehog target genes include *Ptch1* itself, *hedgehog interacting protein (Hhip)* and *Bmps* to name a few (Roberts et al., 1995, Gupta et al., 2010). Interestingly, we showed that redistribution of Ihh from growth plate into the perichondrium in mutant mice and concurrent ectopic expression of *Ptch1* and *Gli1* within the perichondrium itself was followed by ectopic cartilage formation, suggesting that aberrant hedgehog signaling may also cause exostosis formation (Koyama et al., 2007). In good agreement, a recent report on the characterization of a metachondromatosis mouse model described formation of exostosis-like outgrowths protruding from epiphyseal bone that were positive for *Ihh* expression (Kim et al., 2014). Taken together, these studies suggest that ectopic hedgehog signaling and/or BMP signaling could be culprits for excess and ectopic cartilage formation and that inhibiting either or both of these pathways (and preferably the most upstream one) could decrease chondrogenesis and ultimately reduce or prevent exostosis formation and/or growth.

HhAntag is a powerful drug that inhibits hedgehog signaling by blocking the activity of the signaling receptor Smo and has been shown to do so effectively in a variety of normal and cancer cell types, including neuronal and tumorigenic cells (Williams et al., 2003, Romer et al., 2004, Yauch et al., 2008, Scales and de Sauvage, 2009, Chenna et al., 2012, Kunkalla et al., 2013). Thus, we asked here whether HhAntag would inhibit chondrogenesis, whether it could prevent it even during over-stimulation of chondrogenesis by exogenous BMP treatment, and whether its action involved modulation or co-modulation of signaling pathways. The data described here provide strong support for these predictions.

Materials and Methods

Mouse lines, mating, and genotyping

Gli1-LacZ mice were purchased from Jackson labs (Stock No. 008211; Bar Harbor, ME). Male *Gli1-LacZ* mice were mated with female CD-1 mice (Charles River Laboratories). Pregnant mice were sacrificed at embryonic day 12 (E12) by IACUC approved methods. Genotyping was carried out with β-galactosidase staining of tail fragments according to manufacturer's protocol (EMD Millipore; Darmstadt, Germany).

Preparation, treatment, and analysis of micromass cultures

Micromass cultures were prepared from E12 CD-1 mouse embryo limb buds (Ahrens et al., 1979). Briefly, limb bud mesenchyme was dissociated in 0.5% trypsin-EDTA at 37°C. The dissociated cells were suspended at a concentration of 15×10^6 cells/ml in DMEM containing 3% fetal bovine serum and antibiotics. Micromass cultures were initiated by spotting 10 μl of the cell suspensions (1.5×10^5 cells) onto the surface of 12-well tissue culture plates. After a 90 min incubation at 37°C in a humidified CO_2 incubator to allow for cell attachment, the cultures were given 1.0 ml of medium. After 24 h, medium supplemented with HhAntag (0.2 μM, 1.0 μM, or 5.0 μM) (provided as a gift from Genentech; San Francisco, CA), recombinant human BMP-2 (rhBMP-2) (100 ng/ml) (R&D Systems; Minneapolis MN), or a combination of HhAntag (1.0 μM)/rhBMP-2 (100 ng/ml) was added to the cultures. Fresh reagents (drug and/or protein) were given with medium change every third day. Equivalent amounts of vehicle (DMSO) were added to control cultures. Cultures were stained with Alcian blue (pH 1.0) after 4 and 6 days to monitor chondrogenic cell differentiation (Huegel et al., 2013). Images were taken with a Nikon SMZ-U microscope equipped with a SPOT insight camera (Diagnostic Instruments, Inc.; Sterling Heights, MI) and acquired with SPOT 4.0 software. Micromass analysis was performed using ImageJ. Images were made binary under an RGB threshold and "Particle Analysis" was utilized to measure Alcian blue positive area and nodule number (Gutiérrez et al., 2012).

Timed matings were used to collect E12 *Gli1-LacZ* embryonic limb buds for micromass cultures. Cells were plated using the above procedure. In addition to Alcian blue staining, cultures were stained for β-galactosidase after 2, 4, and 9 days to monitor hedgehog activity. For β-galactosidase staining, cultures were washed in 1X phosphate buffered saline (PBS) then fixed in tissue fixative (EMD Millipore, cat no. BG-5-C; Billerica, MA) for 2 min at room temperature. Following fixation, X-gal stock (EMD Millipore, cat no. BG-3-C) diluted in tissue stain base (EMD Millipore, cat no. BG-8-C) was added to the cultures and incubated at 37°C overnight. The following day, cultures were washed in 1X PBS, air dried, and images were taken with a SPOT insight camera operated with SPOT 4.0 software.

Cell viability assay

Cell viability and toxicity were assessed using the LIVE/DEAD® Viability/Cytotoxicity kit (Molecular Probes; Eugene, OR) according to manufacturer's protocol. Briefly, control and HhAntag-treated micromass cultures were incubated with 250 μl of the combined assay reagents: Calcein AM (1 μM) and Ethidium homodimer-1 (EthD-1) (1 μM) for 35 min at room temperature. Images of fluorescent cells were taken with a Nikon Eclipse 7E2000-4 and acquired using Image Pro Plus 7.0 software.

Gene expression analysis

Total RNA was isolated from control and HhAntag-treated micromass cultures on day 4 and 6 using TRIzol reagent according to the manufacturer's protocol. We determined RNA quantification by Nanodrop. One microgram total RNA was reversed transcribed using the Verso cDNA kit (Life Technologies: Thermo Scientific; Carlsbad, CA). Quantitative real-time PCR was carried out using SYBR Green PCR Master Mix in an Applied Biosystems 7500 according to manufacturer's protocol. *Gapdh* was used as the endogenous control and relative expression was calculated using the ΔΔCt method. Real-time PCR was performed using GoTaq DNA Polymerase (Promega; Madison, WI) in a ProFlex PCR system (Applied Biosystems) for 35 cycles. PCR products were resolved on a 2% agarose gel. Bands were normalized to *Gapdh* bands and the intensities were determined by ImageJ. Primer information can be found in Supplemental Table S1.

Protein analysis

Cell lysates from micromass cultures treated with DMSO, HhAntag (1 μM), rhBMP-2 (100 ng/ml) or HhAntag (1 μM)/rhBMP-2 (100 ng/ml) for a period up to four days were lysed in 1X RIPA with protease and phosphatase inhibitors. Lysates were centrifuged at 13,200 rpm at 4°C and supernatants were collected. Protein concentration for each sample was determined by MicroBCA Protein Assay Kit (Pierce, Rockford, IL) according to the manufacturer's protocol. Total cellular proteins (30 μg) were electrophoresed on 4–12% NuPAGE Bis-Tris gel (Life Technologies) and transferred to PVDF membranes (Life Technologies). Membranes were blocked in 1% BSA/1X Tris Buffered Saline/tween 20 (TBST) and incubated overnight at 4°C with phosphoSmad1/5/8 (pSmad1/5/8) (1:1000; Cell Signaling, cat no. 13820; Beverly MA) or phosphop38 (pp38) (1:1000; Cell Signaling, cat no. 4511). Membranes were washed in 1X TBST and incubated with anti rabbit IgG horseradish peroxidase-linked (1:2,000; Cell Signaling, cat no. 7074) for 1 h at room temperature. The antigen-antibody complexes were detected with SuperSignal® West Dura Extended Duration Substrate (Pierce) chemiluminescent detection system. Membranes were re-blotted with Smad 1 (1:1000; Cell Signaling, cat no. 9743) or p38 (1:1000; Cell Signaling cat no. 9212) for normalization. For a loading control, membranes were blotted with Gapdh (1:1000; Santa Cruz Biotechnology, cat no. 32233; Dallas, TX). Band intensities were determined by ImageJ.

Explant cultures

Forelimbs were isolated from E12.5 CD-1 mouse embryos and cultured on Nitex® Nylon filter membranes (Sefar ca no. 03-20/14; Buffalo, NY) in a 24 well plate. The explanted forelimbs were positioned at the air-medium interface using approximately 200 μl of DMEM supplemented with 1% FBS. HhAntag (10 μM or 100 μM) was added directly to the media, and control cultures were treated with DMSO. Explants were cultured for 3 days and then processed for Alcian blue staining. Additional experiments were performed using E16.5 forelimbs. Heparin-coated beads (Sigma, cat no. H-5263; St. Louis, MO) either incubated with rhBMP-2 (1 μg/μl) or DMSO were implanted near the groove of Ranvier of the metacarpals. For administration of HhAntag to the forelimb explant cultures, HhAntag was mixed with Matrigel Matrix GFR (VWR cat no. 47743-718; Radnor, PA) for a total concentration of 10 μM and microinjected at the site of either the DMSO or rhBMP-2 coated bead. Samples were cultured for 6 days and then processed for Alcian blue staining. Images were taken with the Nikon SMZ-U and acquired using SPOT software. Following image acquisition, samples were processed for histology.

Histological staining

Forelimbs from explant cultures were fixed in 4% paraformaldehyde, dehydrated with increasing concentrations of ethanol, cleared in xylene and embedded in paraffin wax. Five micrometer sections were deparaffinized and rehydrated then stained with hematoxylin and eosin. Bright-field images were taken with a SPOT insight camera (Diagnostic Instruments, Inc.) operated with SPOT 4.0 software.

Statistical analysis

Results were analyzed using Prism 6 (GraphPad Software, Inc., La Jolla, CA). Student's *t*-test and One-way ANOVA was used to establish statistical significance. Threshold for significance for all tests was set as $P \leq 0.05$.

Results

HhAntag reduces cartilage nodule formation in vitro

HhAntag has not been previously tested for ability to prevent or inhibit chondrogenesis. To this end, we isolated limb bud mesenchymal cells from E12.0 mouse embryos and seeded them in high-density micromass cultures, a popular experimental system in which the cells undergo chondrogenic cell differentiation and produce cartilage nodules over time (Ahrens et al., 1979). To determine whether and to what extent HhAntag inhibited chondrogenesis, cultures were treated with increasing concentrations of the drug up to 5.0 μM. On day 4, cultures were stained with Alcian blue to detect proteoglycan accumulation and degree of differentiation in HhAntag-treated versus companion control DMSO-treated cultures. Control cultures exhibited numerous well-formed and Alcian blue-positive cartilage nodules (Fig. 1A and B), but there were fewer and fewer positive nodules with increasing HhAntag doses (Fig. 1C–H). Thus, nodule number had decreased substantially in cultures treated with 1.0 μM HhAntag (Fig. 1E and F) and there were virtually no stainable nodules at the highest concentration of 5.0 μM (Fig. 1G and H). Imaging analysis and quantifications showed that Alcian blue staining was significantly reduced in 1.0 μM and 5.0 μM HhAntag-treated versus control cultures (Fig. 1K), and nodule number was significantly decreased by more than 50% in all cultures (Fig. 1L). Counterstaining with hematoxylin showed that cultures treated with 1.0 μM HhAntag was essentially indistinguishable from control cultures indicating that there were no major side effects or cell toxicity (Fig. 1I and J). On the other hand, some of the cultures treated with 5.0 μM HhAntag were uneven and may have experienced some toxic effects (not shown). To further confirm that HhAntag was not toxic to the cells, we performed LIVE/DEAD® Viability/Cytotoxicity assays on control and HhAntag-treated cultures. Indeed, cultures treated with 5.0 μM HhAntag displayed an increased number of positive Ethidium homodimer-D1 labeled cells compared to control and 1.0 μM HhAntag-treated cultures. There was no statistical difference in control versus 1.0 μM HhAntag-treated cultures (Fig. 1M–P). Based on these initial findings, a maximal dose of 1.0 μM HhAntag was used in all subsequent experiments.

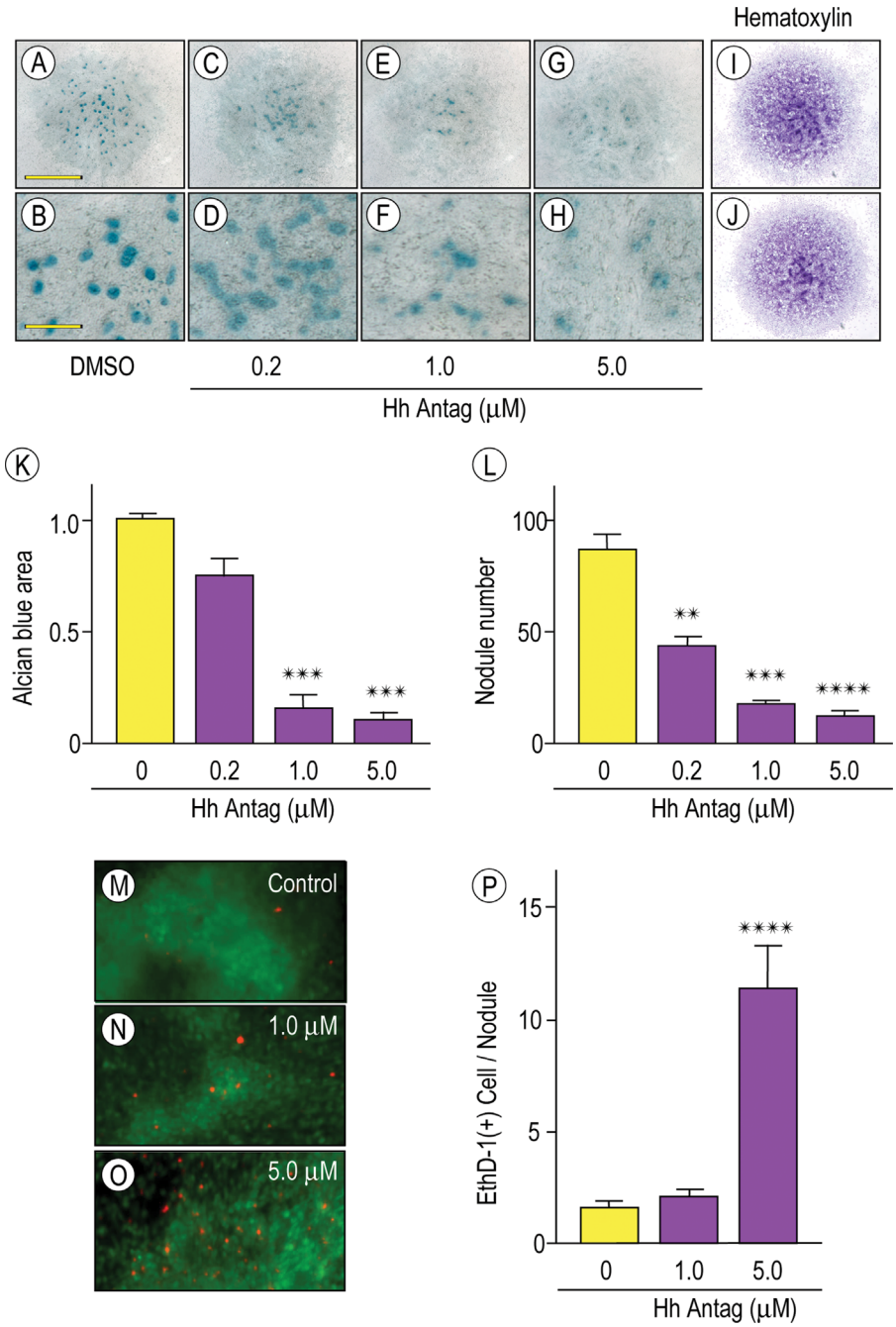

Fig. 1. HhAntag inhibits chondrogenesis dose-dependently. (A, C, E, G) Alcian blue stained day 4 micromass cultures revealing a decrease in cartilage nodule formation with increasing concentrations of HhAntag. (B, D, F, H) Magnified images of A, C, E, and G respectively. (I, J) Control (I) and 1 μM HhAntag (J) -treated cultures counterstained with Hematoxylin. (K, L) Histograms of image assisted quantification of Alcian blue positive area and nodule number in control cultures (yellow) versus cultures treated with indicated concentrations of HhAntag (purple). (M-P) LIVE/DEAD® Cell Viability/Toxicity assay on day 6 control and HhAntag-treated cultures. Magnified images of individual nodules. Calcein AM-labeled cells (green) represent viable cells and Ethidium homodimer-1-labeled cells (red) represent nonviable cells. (O) 5–10 nodules per well were used to calculate the number of ethidium homodimer-1 labeled cells. ($n = 3$; $^{**}P < 0.01$; $^{***}P < 0.001$; $^{****}P < 0.0001$). Graphs depict means ± SEM. Scale bar: 1.5 mm.

Because the micromass cultures continue to develop and mature over time, we assessed the effects of HhAntag on day 6 of culture. Control cultures exhibited a greater number of Alcian blue-staining nodules at day 6 (Fig. 2E and I) compared to day 4 (Fig. 2A), but nodule number was decreased greatly by HhAntag at both time points (Fig. 2B, F, and J). To determine whether HhAntag was able to inhibit chondrogenesis even in the presence of excess pro-chondrogenic factors, we co-treated the cultures with HhAntag and rhBMP-2 and compared the responses to cultures treated with either agent. As expected, rhBMP-2-treated cultures displayed more robust cartilage nodule formation (Fig.2C, G, and K) compared to

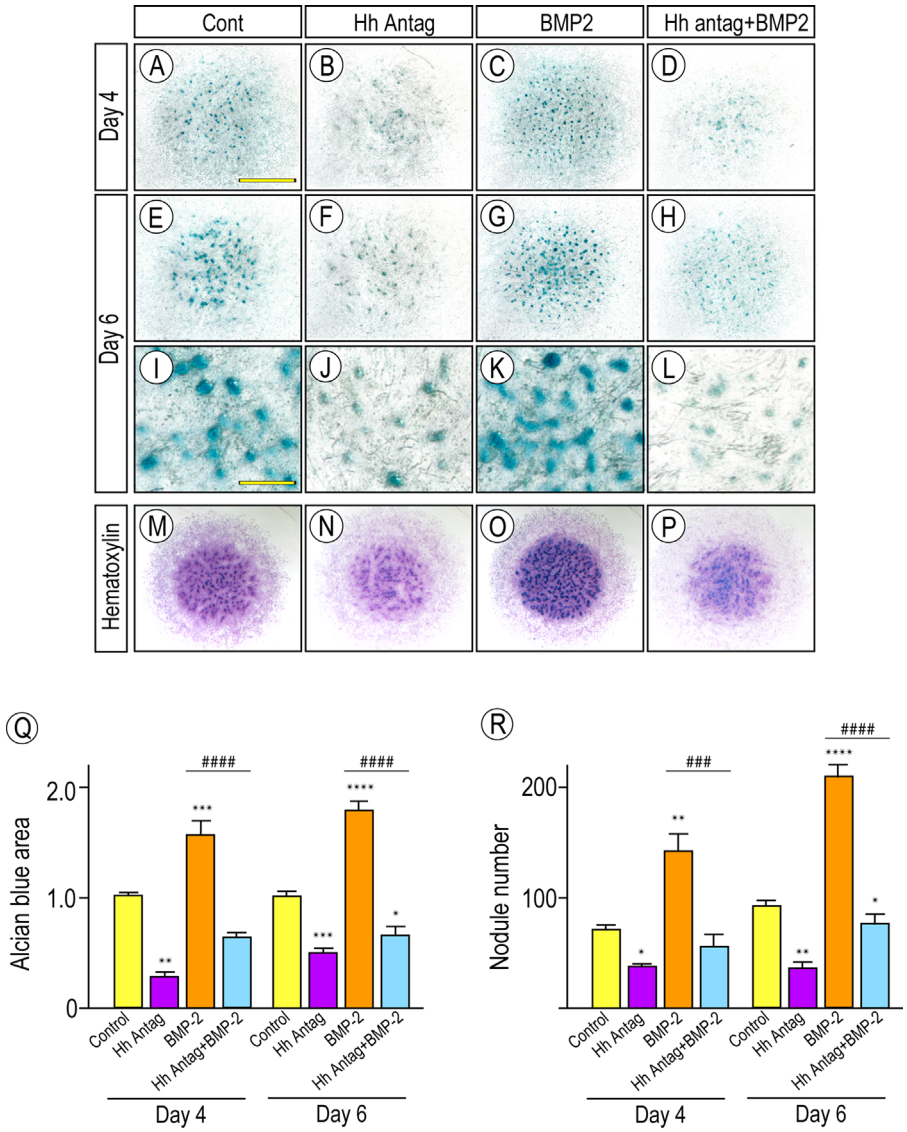

Fig. 2. HhAntag counters the pro-chondrogenic effects of rhBMP-2 in vitro. (A–H) Alcian blue stained day 4 and 6 micromass cultures treated with DMSO, HhAntag (1 μM), rhBMP-2 (100 ng/ml), and HhAntag (1 μM) plus rhBMP-2 (100 ng/ml). Note that HhAntag decreased cartilage nodule both by itself and in cultures co-treated with rhBMP-2 compared to control. rhBMP-2 by itself boosted nodule formation as expected. (I–L) Magnified images of day 6 micromass cultures. (M–P) Day 6 control and treated micromass cultures counterstained with Hematoxylin. (Q, R) Image assisted quantification of Alcian blue positive area and nodule number in control versus treated micromass cultures (n = 6; $^{*}P = 0.05$ $^{**}P < 0.01$; $^{***}P < 0.001$; $^{****}P < 0.0001$; ###$P < 0.001$; #####$P < 0.0001$, where # denotes statistical significant difference between rhBMP-2-and HhAntag/rhBMP-2-treated cultures). Graphs depict means ± SEM. Scale bar: 1.5 mm.

control cultures (Fig. 2A, E, and I). Interestingly, HhAntag was still able to counteract the stimulatory effect of rhBMP-2, and the co-treated cultures had minimal nodule formation (Fig. 2D, H, and L) comparable to that seen in HhAntag-treated cultures (Fig. 2B, F, and J). Counterstaining with hematoxylin showed no obvious change in overall cell population (Fig. 2 M–P). Image analysis for Alcian blue area and nodule number at day 4 and 6 revealed a significant reduction in both parameters in HhAntag-treated and HhAntag/rhBMP-2-co-treated cultures compared to control and rhBMP-2-treated cultures, respectively (Fig. 2Q and R). The ability of HhAntag to inhibit chondrogenesis is reminiscent of the effects seen previously with another hedgehog antagonist -Cyclopamine- that was tested in rabbit bone marrow cells and limb mesenchymal cells in vitro (Bruce et al., 2010, Wu et al., 2013).

HhAntag downregulates key chondrogenic genes

To verify and extend the data above, we assessed the expression of key chondrogenic genes in control and HhAntag-treated cultures. Total RNAs extracted from day 4 and 6 cultures were processed for quantitative PCR analysis. We found that *Sox9*, a master regulator of chondrogenesis (Lefebvre and de Crombrugghe 1998), was significantly downregulated by HhAntag treatment at both time points (Fig. 3A and B). Differentiated chondrocytes synthesize and accumulate large amounts of extracellular matrix responsible for the Alcian blue staining as shown in control micromass cultures above. qPCR analysis indicated that expression of two abundant matrix components -*aggrecan* (*Acan*) and *type II collagen* (*Col2a1*)- was significantly downregulated by HhAntag-treated cultures. Lastly,

we assessed the expression levels of *runt related transcription factor 2* (*Runx2*), a marker of chondrocyte hypertrophy and endochondral ossification. Day 4 HhAntag-treated cultures exhibited a significant decrease in *Runx2* expression. This trend was also seen in day 6 HhAntag-treated cultures, but was not significant (Fig 3A and B).

Patterns of hedgehog signaling, downstream effectors, and interference by HhAntag

Exogenous hedgehog proteins are capable of promoting chondrogenic cell differentiation in vitro (Enomoto-Iwamoto et al., 2000), but less is known about endogenous hedgehog signaling during this process. Thus, we set up micromass cultures prepared from the limb buds of heterozygous E12.0 *Gli1-LacZ* mouse embryos that carry a β-galactosidase knock-in reporter into the *Gli1* locus and are widely used as a read-out of hedgehog signaling (Ahn and Joyner, 2004). Some cultures were left untreated, and companion cultures were treated with HhAntag and/or rhBMP-2 and processed for LacZ staining over culture time. In control cultures and those treated with rhBMP-2, LacZ staining was already appreciable at day 2 within incipient prechondrogenic nodule-like cell condensations and exhibited a diffuse and uniform pattern (Fig. 4A and C) suggesting that endogenous hedgehog signaling is activated early in chondrogenesis. By day 4 and 9, LacZ staining had become very strong and was even more so in rhBMP-2-treated cultures (Fig. 4E, G, I, and K) mirroring the formation of cartilage nodules and their increase over time and rhBMP-2 treatment. Interestingly, staining was often prominent along the periphery of each nodule producing a donut-like staining pattern (Fig. 4E and G, insets) indicating that hedgehog proteins diffused away from the nodule cartilaginous core into surrounding cells as they are known to do in vivo as well (Vortkamp et al., 1996). At each time point examined, LacZ staining was dramatically reduced following HhAntag and regardless of whether the cultures had been co-treated with rhBMP-2 (Fig. 4B, D, F, H, J, and L), indicating that HhAntag was indeed acting as a potent inhibitor of hedgehog signaling in the micromass cultures. Quantification by image analysis showed that the number of LacZ positive nodules was significantly reduced in all HhAntag-treated cultures and at each time point examined (Fig. 4Q). Hematoxylin counterstaining showed typical distribution of cells in all cultures, with more cells present in the center and fewer in the periphery in both untreated and treated cultures (Fig. 4M–P).

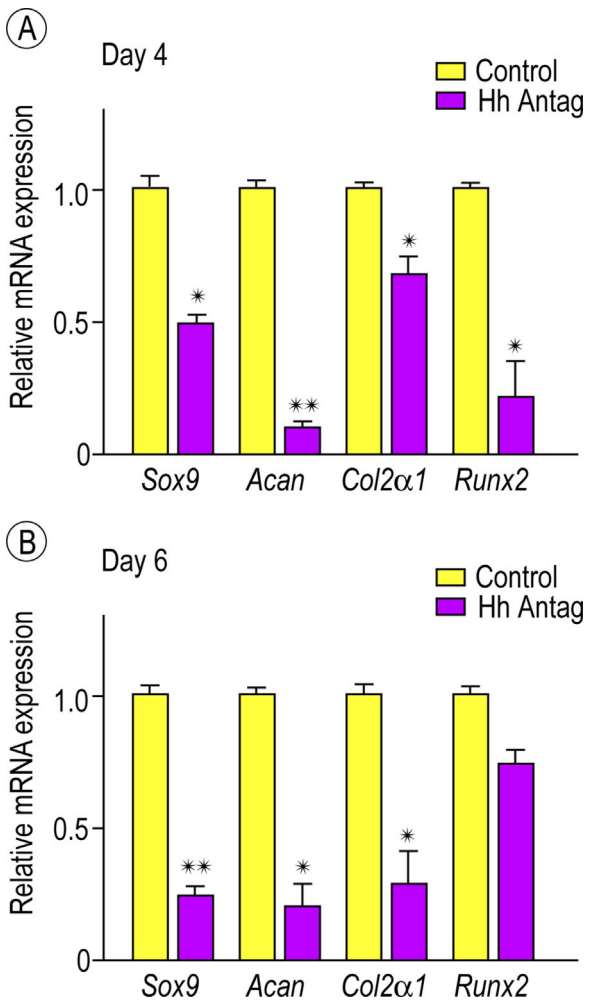

Fig. 3. Gene expression of chondrogenic markers is decreased in HhAntag-treated cultures. (A, B) Histograms depicting the relative expression levels of *Sox9*, *Acan*, *Col2α1*, and *Runx2* that were all decreased in day 4 and day 6 HhAntag-treated cultures compared to respective control cultures ($n = 3$; $^{*}P < 0.05$; $^{**}P < 0.01$). Graphs depict means ± SEM.

To extend the data and gain more insights into mechanisms, we evaluated the expression patterns of downstream signaling molecules of the hedgehog pathway. HhAntag is known to antagonize hedgehog signaling by binding to the Smo receptor, thereby preventing further downstream signaling and activation of target genes such as the Gli family of transcription factors Gli1, Gli2, and Gli3 (Yauch et al., 2008). The Gli proteins play a cooperative but also complex role in modulating the expression of target genes including *Ptch1* and *Hhip* that in turn affect hedgehog signaling (Chuang and McMahon, 1999). To examine whether and which genes of the hedgehog pathway may be affected by HhAntag, we performed hedgehog signaling PCR arrays with RNAs isolated from day 4 and 6 control versus treated micromass cultures. This analysis showed a concerted downregulation of several hedgehog target genes including *Gli1*, *Hhip,* and *Ptch1* as well as several *Bmp* and *Wnt* ligands (see Supplemental Table S2 for additional genes examined). Following PCR array analysis, we performed qPCR to verify key results. Expression of *Gli1*, a direct target of hedgehog signaling that in turn activates other target genes, was barely detectable in all HhAntag-treated cultures compared to control cultures at both day 4 and 6 (Fig. 5A and B). *Gli2* and *Gli3* are normally expressed in the absence of hedgehog signaling, but both genes were downregulated as well in the presence of the inhibitor, suggesting that interference with Smo signaling affects Gli2 and Gli3 also. *Hhip*, a membrane-bound glycoprotein that interacts with the hedgehog proteins to attenuate their action and whose expression is activated by hedgehog signaling (Chuang and McMahon, 1999), was significantly down-regulated in HhAntag-treated cultures. *Ptch1*, another target gene in the pathway whose roles is to sequester hedgehog proteins thereby limiting their action on target cells and also to transduce hedgehog signaling (Chen and Struhl, 1996), was also significantly downregulated in HhAntag-treated cultures (Fig. 5A and B). Additionally, we examined *Pthrp*, which cooperates with Ihh to regulate chondrocyte proliferation and differentiation (Vortkamp et al., 1996). *Pthrp* expression also was significantly decreased in HhAntag-treated cultures at both day 4 and 6 of culture (Fig. 5A and B) suggesting that the *Pthrp-Ihh* loop may have been interrupted (Kronenberg, 2003). In addition to analysis

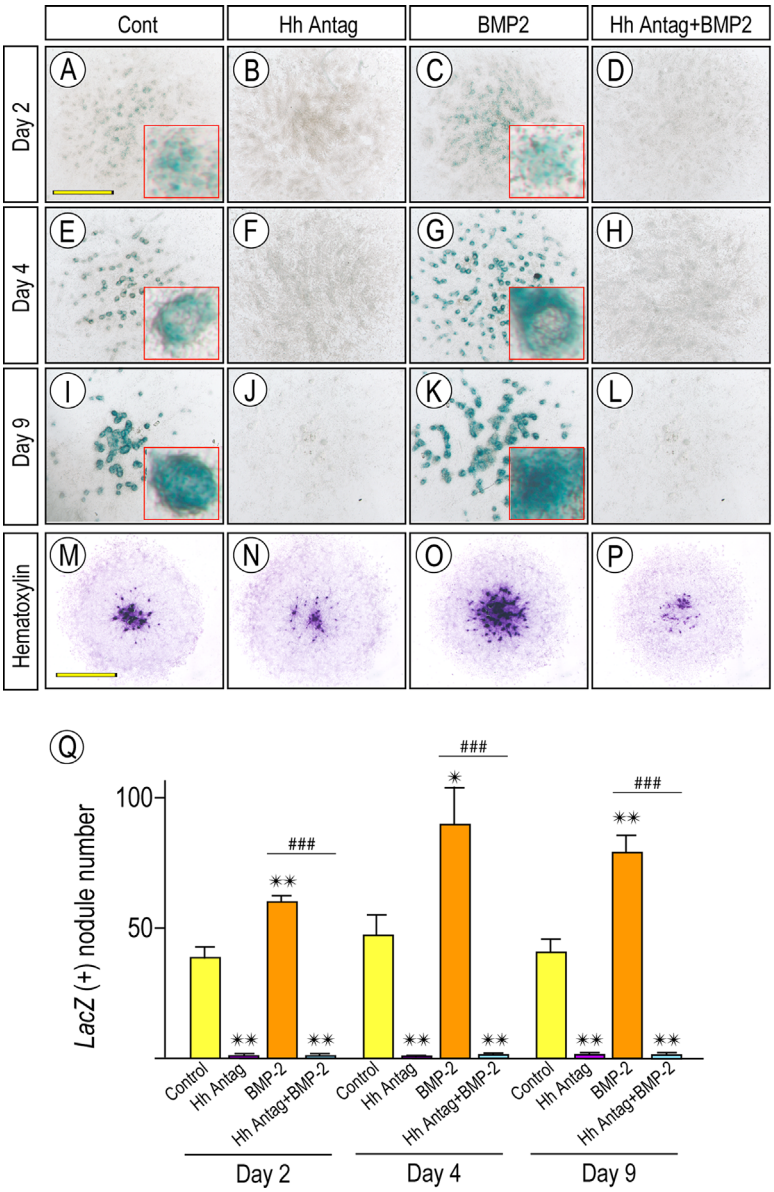

Fig. 4. Hedgehog signaling activity is inhibited by HhAntag. (A–D) β-galactosidase staining of day 2 control and treated micromass cultures. Both control and rhBMP-2 (100 ng/ml)-treated cultures already display β-galactosidase staining through the incipient pre-chondrogenic nodules, but this early signaling activity is blocked in HhAntag-treated (1 μM) and HhAntag (1 μM)/rhBMP-2 (100 ng/ml)-co-treated cultures. (E–H) β-galactosidase staining of day 4 control and treated micromass cultures showing that staining was very strong in control and rhBMP-2 treated cultures, but essentially undetectable in HhAntag- and HhAntag/rhBMP-2-treated cultures. Note that the staining in control and rhBMP-2-treated cultures was particularly strong around the perimeter of the cartilage nodules. (I–L) β-galactosidase staining patterns of Day 9 control and treated micromass cultures that are similar to those seen at day 4. Control and rhBMP-2 treated cultures revealed β-galactosidase staining within the nodules as well as along the periphery of the nodules. Insets surrounded by a red box depict pre-chondrogenic and chondrogenic nodules from each respective culture at higher magnification. (M–P) Hematoxylin staining of control and treated micromass cultures. (Q) Histograms showing image assisted quantification of LacZ positive nodule number in control versus treated micromass cultures (n = 3; $^{*}P < 0.05$; $^{**}P < 0.01$; ###$P < 0.001$, where # denotes statistical significant difference between the rhBMP-2-and HhAntag/rhBMP-2-treated cultures). Graphs depict means ± SEM. Scale bar: 1.5 mm.

of downstream signaling molecules, we performed real time PCR on control and HhAntag-treated micromass cultures to evaluate mRNA expression of *Shh*, *Ihh*, and *Dhh*. *Shh* was not detectable in our micromass cultures (Supplemental Fig. S1). Interestingly, in the HhAntag-treated cultures *Ihh* expression was upregulated by 2.5-fold compared to the control cultures at day 4. By day 6 *Ihh* expression decreased in both control and HhAntag-treated cultures (Fig. 5C and D). Even more strikingly was *Dhh* expression in the HhAntag-treated cultures, which were upregulated by almost fourfold compared to control cultures and persisted to day 6 (Fig. 5C and E).

HhAntag modulates BMP ligand expression and signaling

Studies have shown that Ihh regulates gene expression of several BMPs (Pathi et al., 1999, Kawai and Sugiura, 2001). Therefore we asked whether expression of such genes would

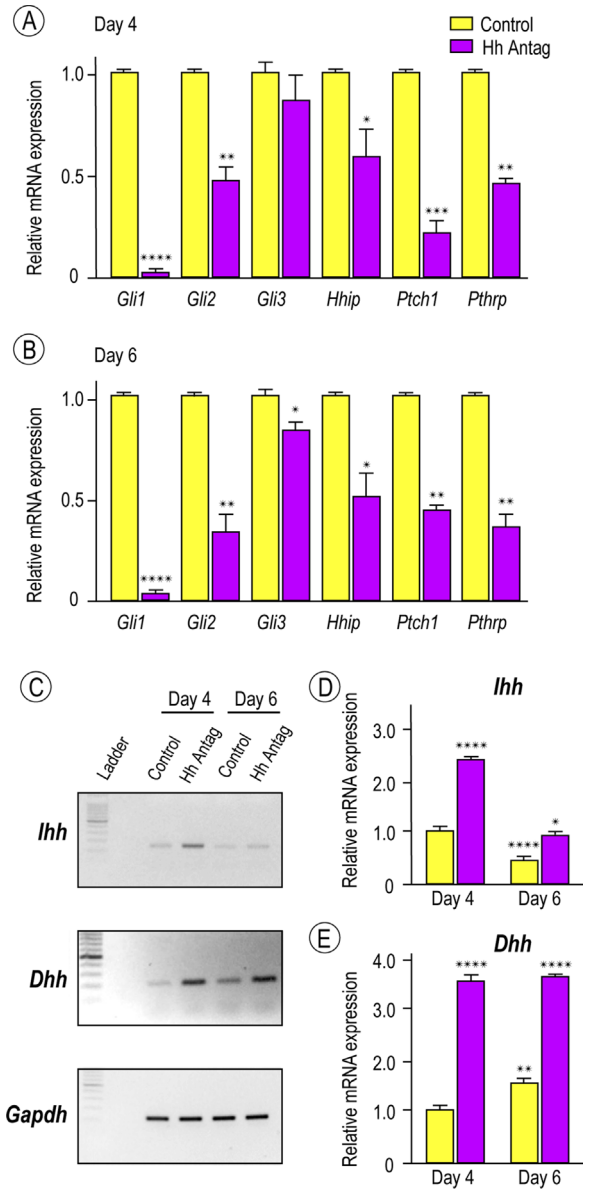

Fig. 5. Gene expression for hedgehog target genes is decreased in HhAntag-treated cultures. (A, B) Histograms depicting the relative expression of *Gli1*, *Gli2*, *Gli3*, *Hhip*, *Ptch1*, and *Pthrp* and showing that they were all decreased in HhAntag-treated cultures compared to control cultures at day 4 and 6. (C) Gene expression for *Ihh* and *Dhh* is upregulated in HhAntag-treated cultures at day 4 and 6. Bands were normalized to *Gapdh* and quantified in D and E. (n = 3; $^{*}P < 0.05$; $^{**}P < 0.01$; $^{***}P < 0.001$; $^{****}P < 0.0001$). Graphs depict means ± SEM.

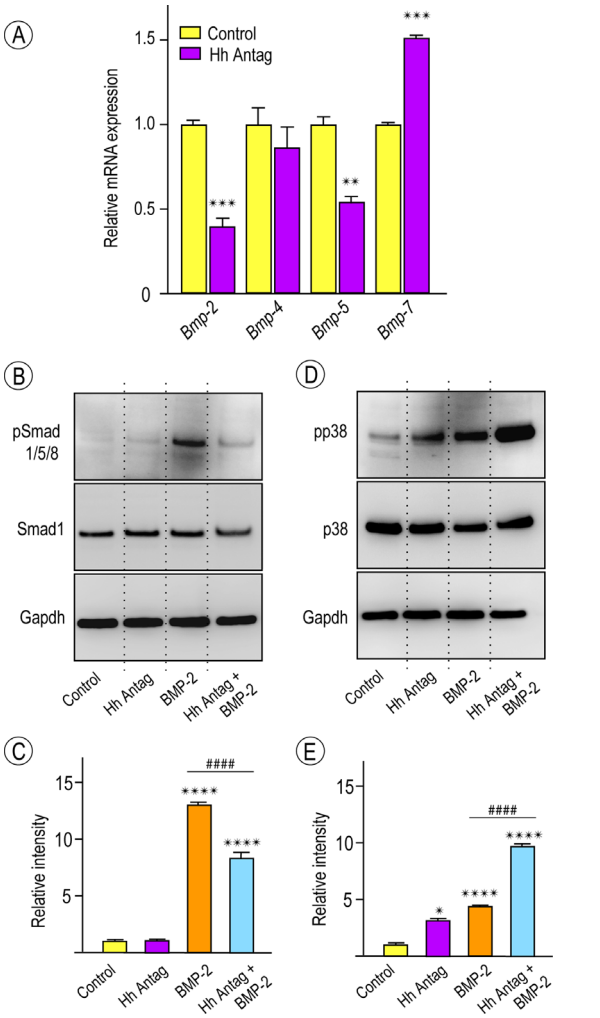

Fig. 6. HhAntag treatment modulates BMP gene expression and signaling. (A) Histograms showing that gene expression of *Bmp-2* and *Bmp-5* was significantly downregulated in HhAntag-treated (1 μM) cultures compared to control cultures, but *Bmp-4* gene expression was mildly affected and *Bmp-7* expression was significantly up-regulated by HhAntag. (n = 3; $^{**}P < 0.01$; $^{***}P < 0.001$). (B) Representative immunoblots for pSmad1/5/8 and Smad 1 protein levels using 30 μg total protein from micromass cultures treated as indicated for 1 h. Note that pSmad1/5/8 levels remained largely unchanged in control and HhAntag-treated (1 μM) cultures, but were markedly increased in rhBMP-2 (100 ng/ml)- and HhAntag (1 μM)/rhBMP-2 (100 ng/ml)-treated cultures. Membranes were reblotted with Smad 1 for sample loading normalization. (C) Normalized band intensity quantification of blots in (B) with the control set at 1. (D) Representative immunoblots for pp38 and p38 protein levels using 30 μg total protein from micromass cultures treated as indicated for 1 h. All treatment groups displayed an increase in pp38 protein levels compared to control, but this increase was particularly prominent in the HhAntag/rhBMP-2 co-treated cultures. Membranes were reblotted with p38 for sample loading normalization. (E) Normalized band intensity quantification of blots in (D) with the control set at 1. Gapdh served as a loading control for both blots. (n = 3; $^{*}P < 0.05$; $^{****}P < 0.0001$; ####$P < 0.0001$, where # denotes statistical significant difference between rhBMP-2-and HhAntag/rhBMP-2-treated groups). Graphs depict means ± SEM.

change during HhAntag treatment of micromass cultures. qPCR analysis indicated that expression of both *Bmp-2* and *Bmp-5* was indeed significantly downregulated in HhAntag-treated versus control cultures (Fig. 6A). In comparison, expression of *Bmp-4* was minimally affected while *Bmp-7* expression was actually up-regulated (Fig. 6A), indicating that the roles of hedgehog signaling in *Bmp* expression during chondrogenesis are complex and that the *Bmp7* up-regulation may be compensatory.

Because addition of rhBMP-2 did not rescue the inhibition of chondrogenesis elicited by HhAntag as shown above, we asked whether this was occurring at the level of BMP signaling or at a different regulatory level. Control cultures and cultures treated with HhAntag-, rhBMP-2-, and HhAntag plus rhBMP-2 on day 4 were processed for cell lysate preparation and

immunoblot analysis of canonical and non-canonical BMP signaling activities. It should be noted that these day 4 cultures had received the last addition of fresh reagents on day 3. Immunoblot analysis showed that there were no obvious changes in the levels of pSmad1/5/8 or pp38 in these cultures (data not shown). Thus, all the day 4 cultures were given fresh medium containing freshly added DMSO (control), HhAntag, rhBMP-2, or HhAntag plus rhBMP-2 to determine how the cells would respond to acute exposure to each condition. Cultures were then lysed 1 h later, and the resulting homogenates were processed for immunoblot as above. Control cultures responded minimally to the medium change and their levels of pSmad1/5/8 and pp38 did not change appreciably, while the pp38 levels had increased moderately in HhAntag cultures (Fig. 6B–E). Interestingly, the levels of both pSmad1/5/8 and pp38 increased several folds in rhBMP-2 and HhAntag/rhBMP-2-treated cultures (Fig. 6B–E), and the increase in pp38 was particularly prominent in the HhAntag/rhBMP-2-treated cultures, amounting to nearly 10-fold over control value (Fig. 6D and E). The data indicate that HhAntag modulated canonical and noncanonical BMP signaling.

Chondrogenesis is reduced in forelimb explants in the presence of HhAntag

To make sure that HhAntag has similar effects when tested in an experimental condition closer to an in vivo condition, we tested its effects in explants. Thus, we isolated the entire forelimb autopod regions from E12.5 mouse embryos and maintained them in organ culture in medium containing vehicle (DMSO), 10 μM or 100 μM HhAntag. By day 3 the control explants displayed well-formed cartilaginous phalanges (Fig. 7B, arrowheads) that stained strongly with Alcian blue, were separated by incipient synovial joints and had progressed much in development as compared to the barely appreciable digit anlagen present in freshly-isolated E12.5 explants at time 0 (Fig. 7A). In line with its effects in micromass cultures, HhAntag effectively hampered the development of the digit structures such that they were much reduced in 10 μM HhAntag-treated explants (Fig. 7C) and virtually absent in 100 μM-treated explants (Fig. 7D). This is closely reminiscent of the thin, small, and under-developed cartilaginous skeletal elements previously described in *Ihh* mutant mice (St-Jacques et al., 1999).

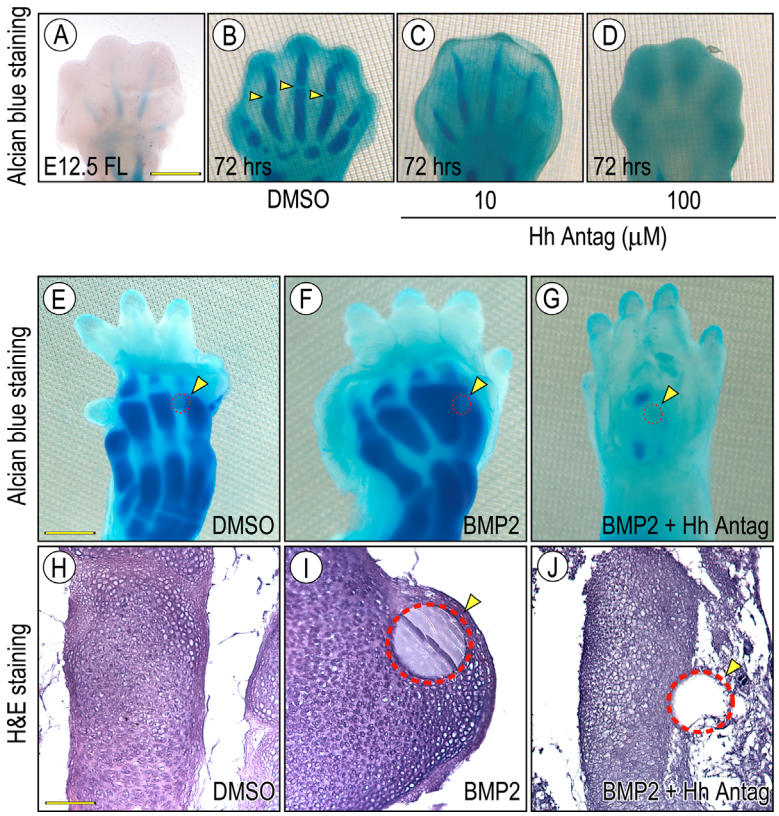

Fig. 7. HhAntag prevents rhBMP-2-induced ectopic chondrogenesis in forelimb explants. (A) Alcian blue staining of a freshly-isolated E12.5 forelimb without culturing. (B–D) E12.5 forelimbs in explant cultures treated with DMSO (control) (B), HhAntag (10 μM) (C) or HhAntag (100 μM) (D) for 72 h and then stained with Alcian blue. Note that forelimbs treated with 10 μM HhAntag show thinner cartilaginous digits and incomplete joint cavitation compared to control, and forelimbs treated with 100 μM HhAntag exhibit barely visible digits condensations. (E–G) Alcian blue stained E16 forelimbs that were implanted with beads coated with DMSO (control) (E), rhBMP-2 (1 μg/μl) (F), or HhAntag(10 μM)/rhBMP-2 (1 μg/μl) (G) near the third metacarpal. Yellow arrowheads depict approximate implantation site. Explants were cultured for 6 days and then stained with Alcian blue. Note that the metacarpal implanted with rhBMP-2-coated bead displays ectopic cartilage formation (F, arrowhead) compared to control (E, arrowhead), but co-treatment with HhAntag prevented cartilage growth, both basal and rhBMP-2 stimulated (G, arrowhead). (H–J) Histological sections prepared from (E, F, and G) and stained with Hematoxylin and eosin. (H) Control elements exhibit normal chondrocyte morphology, and those implanted rhBMP-2-coated beads (shown in I, arrowhead) reveal excess and exostosis-like tissue formation completely surrounding the bead. (J) Implantation with rhBMP-2-coated bead plus HhAntag (arrowhead) treatment reduced overall development and growth of the cartilaginous elements. Scale bar: (A–D) 250 μm, (E–G) 500 μm, and (H–J) 150 μm.

To see whether HhAntag would be able to counter ectopic cartilage formation as well, we first established an organ culture system to induce excess chondrogenesis. Thus, we implanted beads pre-coated with rhBMP-2 or DMSO (control) in close proximity of the presumptive cartilaginous metacarpal elements in E16.5 explants. After bead implantation, half of the explants receiving the rhBMP-2-coated beads were microinjected with 3–5 μl HhAntag (10 μM) into the same region. After 6 days, the explants were stained with Alcian blue. Indeed, we observed very enlarged cartilaginous elements at/near the site of rhBMP-2 bead implantation (Fig.7F, arrowhead), while the remaining elements were more comparable to those in control cultures (Fig. 7E, arrowhead). Analysis of hematoxylin-eosin stained longitudinal sections showed that control metacarpal elements were composed of typical chondrocytes organized in zones of growth plate and the border between cartilage and surrounding perichondrial tissues was uniform and linear as expected (Fig. 7H). In the rhBMP-2-implanted site, however, there was clear formation of excess cartilage that protruded away from the native cartilaginous element and distorted the cartilage-perichondrial border (Fig. 7I), reminiscent of what is seen at the early stages of exostosis formation in vivo (Huegel et al., 2013). When we examined the specimens receiving rhBMP-2 plus HhAntag, we observed a sharp inhibition of cartilage development both near and around the site of bead implantation and thus, full prevention of excess cartilage formation (Fig. 7G, arrowhead and J).

Discussion

Our results provide evidence that HhAntag is a potent inhibitor of chondrogenic differentiation of limb bud mesenchymal cells in micromass culture as indicated by marked reductions in cartilage nodule formation, Alcian blue staining, and expression of cartilage gene markers and master regulators. The data suggest that HhAntag's action includes its ability to mitigate and limit the roles of the canonical and non-canonical BMP signaling pathways both of which are known to normally have pro-chondrogenic effects (Wan and Cao, 2005). We observe strong inhibition of chondrogenesis by HhAntag even in explant cultures, a condition in which the progenitor cells retain their native tissue organization and structure and which approximates more closely the in vivo condition. It appears then that the hedgehog and BMP signaling pathways may act in parallel or may converge on downstream target(s) during chondrogenesis and could be targeted to limit excess cartilage formation in pathologies such as HME.

The data suggest two means by which HhAntag could inhibit chondrogenesis. The first would be a direct down-regulation of *Sox9* expression via suppression of *Gli1* expression as our data indicate. Sox9 is an essential transcription factor for chondrogenesis and directly activates other chondrogenic genes, such as *Col2α1* (Lefebvre and de Crombrugghe, 1998). Interestingly, there is a direct physical interaction between Gli1 and Sox9, and Gli1 directly binds to the *Sox9* promoter thereby regulating *Sox9* gene activity (Bien-Willner et al., 2007). In line with our findings, a previous study described the absence in tracheal cartilage formation in *Shh* mutants due to lack of *Sox9* and *Gli1* gene expression (Park et al., 2010). Thus, the inhibition of hedgehog signaling and Smo activity by HhAntag could cause down-regulation of *Sox9* expression through *Gli1* expression, leading to reduced chondrogenesis. Additional experiments are needed to fully establish a direct relationship between *Sox9* and *Gli1*.

In addition to a direct effect, our data support an indirect route involving a regulatory role of hedgehog signaling in BMP signaling and in turn chondrogenesis. Studies have shown that there is a positive feedback loop between Ihh signaling and BMP expression/action during chondrogenesis. For instance, mis-expression of *Ihh* in the developing limb leads to an up-regulation of BMPs in adjacent perichondrium and proliferating chondrocytes (Pathi et al., 1999, Minina et al., 2001). Additionally, Gli proteins induce BMP expression by up-regulating the promoter activity of BMP genes (Kawai and Sugiura, 2001), and BMP signaling stimulates *Ihh* expression by influencing *Ihh* promoter activity (Seki and Hata, 2004). Currently there is some controversial and conflicting data as to whether Ihh or BMPs lie downstream of each other's function during chondrocyte proliferation and hypertrophic differentiation and whether hedgehog signaling alters BMP signaling during early stages of chondrogenesis (Zou et al., 1997, Minina et al., 2001). Our data indicate that HhAntag reduces chondrogenesis and cartilage formation even in the presence of rhBMP-2 (which by itself greatly stimulates both) and that the inhibitory action of HhAntag involves modulation of canonical and non-canonical BMP signaling effects. Indeed, when the micromass cultures were acutely exposed to fresh HhAntag plus rhBMP-2, they mounted a very strong—and likely compensatory—up-regulation of pSmad1/5/8 and pp38 levels but to no avail since chondrogenesis remained suppressed. It is important to note that we did observe an upregulation in *Ihh* and *Dhh* mRNA expression in HhAntag-treated cultures, which mirrors the increase in pp38. Since the canonical BMP signaling pathway is being suppressed in the HhAntag-treated cultures, it is possible that the cells attempt to compensate by producing more Hh proteins and activating the noncanonical pathway. Together, the data indicate that HhAntag action, and by extension hedgehog signaling, lies parallel of BMP signaling or converge on a downstream target(s). The data lead us to conclude that HhAntag inhibits chondrogenesis by a dual action involving: 1) a direct down-regulation of *Gli1* expression and subsequent reduction of *Sox9* expression and 2) an indirect mode by decreasing *Bmp* expression and eliciting ineffectual action by canonical and non-canonical BMP signaling.

Studies have shown that excess hedgehog signaling in mesenchymal cells and tissues can lead to ectopic and excess cartilage and bone formation in vivo (Koyama et al., 2007, Regard et al., 2013, Kim et al., 2014). In the case of HME, cells including growth plate chondrocytes and perichondrial cells are deficient in HS, and previous studies have shown that a deficiency in HS in the growth plate allows for broader diffusion and distribution of Ihh produced by prehypertrophic chondrocytes (Koziel et al., 2004) that could diffuse into perichondrium, activate signaling in chondroprogenitor cells and result in exostosis formation (Koyama et al., 2007). The organization of an exostosis resembles a miniature epiphyseal growth plate that protrudes away from the lateral surface of skeletal elements such as a long bone and displays a thick perichondrium surrounding the cartilage cap (Hameetman and Bovée, 2003). We have previously shown using conditional *Ext1* mouse mutants that BMP signaling is ectopically elevated along the perichondrium of targeted mutant long bones and is followed by exostosis-like tissue formation violating the chondro-perichondrial boundary (Huegel et al., 2013). This is in line with our findings here that implantation of rhBMP-2-coated beads along metacarpal elements induces excess cartilage formation and emergence of an exostosis-like structure covered by a thick apical perichondrium. Together, the data do suggest that by directly and indirectly hampering the hedgehog and BMP signaling pathways, HhAntag could have encompassing and effective action and inhibit the initiation of chondrogenic differentiation and cartilage and exostosis formation.

No new exostoses form once the growth plates close at the end of puberty (Goud et al., 2012), but pre-existing exostoses may continue to grow and elicit further pathological consequences. In addition, the exostoses –which are initially

benign in nature- can actually undergo malignant transformation and progress to malignant chondrosarcomas, thus becoming life threatening. Thus, there is an urgent need to stop exostosis formation, their further growth, and/or their malignant transformation. As previously mentioned, exostoses resemble growth plates structurally and functionally, and the exostosis chondrocytes express typical markers of growth plate zones (Huegel et al., 2013). Thus, HhAntag could potentially interfere with another essential regulatory mechanism operating in growth plates and specifically the Ihh/Pthrp feedback loop as indicated above (Kronenberg, 2003). This loop regulates the overall rates of chondrocyte proliferation and hypertrophy in growth plate but when altered by gene ablation of *Pthrp* or *Pthrp-R*, causes premature hypertrophy, proliferation stoppage and growth plate closure (Karaplis et al., 1994, Lanske et al., 1996). Our qPCR data show that HhAntag treatment caused a significant reduction in *Pthrp* gene expression. It is possible then that HhAntag could represent a tool by which exostosis chondrocytes could be induced to undergo precocious hypertrophy and cell cycle quiescence, thus reducing further exostosis outgrowth, provoking exostosis involution, and reducing the chance of malignant transformation. Though plausible, this possibility has to be considered cautiously in view of the fact that HhAntag administered to young postnatal mice was found to cause premature closure of the growth plates and lead to growth retardation (Kimura et al., 2008). Thus, administering it to young adolescents can have significant and unwanted side effects on skeletal growth, but such effects should be much milder once skeletal maturity has been reached. Indeed, blockage of hedgehog signaling by genetic means or pharmacological inhibitors was used to treat experimental osteoarthritis in adult mice and no major side effects on skeletal growth were described (Lin et al., 2009). Taken together, our findings and those studies support the possibility that HhAntag or similar hedgehog antagonists could be used to reduce further growth of pre-existing exostoses where they would interfere with the Ihh-Pthrp loop, provoke proliferation arrest, and precocious hypertrophy and reduce the chance of malignant transformation, all actions that could benefit from HhAntag's ability to suppress BMP and hedgehog signaling as well.

Acknowledgements

The study was supported by the NIAMS grant R01AR061758 to MP and EK. We would like to thank Cheri Saunders for technical assistance. We would like to express our gratitude to Genentech Inc. for providing HhAntag. We also acknowledge the passionate efforts of the Multiple Hereditary Exostoses Research Foundation, an organization dedicated to the support of families and patients with MHE and for advocating MHE public awareness and biomedical research.

Literature Cited

Ahn J, Ludecke HJ, Lindow S, Horton WA, Lee B, Wagner MJ, Horsthemke B, Wells DE. 1995. Cloning of the putative tumour suppressor gene for hereditary multiple exostoses (Ext1). Nat Genet 11:137–143.

Ahn S, Joyner AL. 2004. Dynamic changes in the response of cells to positive hedgehog signaling during mouse limb patterning. Cell 118:505–516.

Ahrens PB, Solursh M, Reiter RS, Singley CT. 1979. Position-related capacity for differentiation of limb mesenchyme in cell culture. Dev Biol 69:436–450.

Bernfield M, Gotte M, Park PW, Reizes O, Fitzgerald ML, Lincecum J, Zako M. 1999. Functions of cell surface heparan sulfate proteoglycans. Annu Rev Biochem 68:729–777.

Bien-Willner GA, Stankiewicz P, Lupski JR. 2007. Sox9cre1, a cis-acting regulatory element located 1.1 mb upstream of Sox9, mediates its enhancement through the Shh pathway. Hum Mol Genet 16:1143–1156.

Björnsson J, McLeod RA, Unni KK, Ilstrup DM, Pritchard DJ. 1998. Primary chondrosarcoma of long bones and limb girdles. Cancer 83:2105–2119.

Bruce SJ, Butterfield NC, Metzis V, Town L, McGlinn E, Wicking C. 2010. Inactivation of Patched1 in the mouse limb has novel inhibitory effects on the chondrogenic program. J Biol Chem 285:27967–27981.

Chen Y, Struhl G. 1996. Dual roles for patched in sequestering and transducing hedgehog. Cell 87:553–563.

Chenna V, Hu C, Pramanik D, Aftab BT, Karikari C, Campbell NR, Hong SM, Zhao M, Rudek MA, Khan SR, Rudin CM, Maitra A. 2012. A polymeric nanoparticle encapsulated small-molecule inhibitor of hedgehog signaling (NanoHHI) bypasses secondary mutational resistance to smoothened antagonists. Mol Cancer Ther 11:165–173.

Chuang PT, McMahon A P. 1999. Vertebrate hedgehog signalling modulated by induction of a hedgehog-binding protein. Nature 397:617–621.

Enomoto-Iwamoto M, Nakamura T, Aikawa T, Higuchi Y, Yuasa T, Yamaguchi A, Nohno T, Noji S, Matsuya T, Kurisu K, Koyama E, Pacifici M, Iwamoto M. 2000. Hedgehog proteins stimulate chondrogenic cell differentiation and cartilage formation. J Bone Miner Res 15:1659–1668.

Goud AL, de Lange J, Scholtes VA, Bulstra SK, Ham SJ. 2012. Pain, physical and social functioning, and quality of life in individuals with multiple hereditary exostoses in the Netherlands: A national cohort study. J Bone Joint Surg Am 94:1013–1020.

Gupta S, Takebe N, Lorusso P. 2010. Targeting the hedgehog pathway in cancer. Ther Adv Med Oncol 2:237–250.

Gutiérrez ML, Guevara J, Barrera LA. 2012. Semi-automatic grading system in histologic and immunohistochemistry analysis to evaluate in vitro chondrogenesis. Universitas Scientiarum 17:167–178.

Hameetman L, Bovée JV. 2003. Bone: Osteochondroma. Atlas Genet Cytogenet Oncol Haematol 7:42–44.

Hecht JT, Hayes E, Haynes R, Cole WG, Long RJ, Farach-Carson MC, Carson DD. 2005. Differentiation-induced loss of heparan sulfate in human exostosis derived chondrocytes. Differentiation 73:212–221.

Huegel J, Mundy C, Sgariglia F, Nygren P, Billings PC, Yamaguchi Y, Koyama E, Pacifici M. 2013. Perichondrium phenotype and border function are regulated by Ext1 and heparan sulfate in developing long bones: A mechanism likely deranged in hereditary multiple exostoses. Dev Biol 377:100–112.

Jiao X, Billings PC, O'Connell MP, Kaplan FS, Shore EM, Glaser DL. 2007. Heparan sulfate proteoglycans (HSPGs) modulate BMP2 osteogenic bioactivity in C2C12 cells. J Biol Chem 282:1080–1086.

Karaplis AC, Luz A, Glowacki J, Bronson RT, Tybulewicz VL, Kronenberg HM, Mulligan RC. 1994. Lethal skeletal dysplasia from targeted disruption of the parathyroid hormone-related peptide gene. Genes Dev 8:277–289.

Kawai S, Sugiura T. 2001. Characterization of human bone morphogenetic protein (bmp)-4 and -7 gene promoters: Activation of bmp promoters by gli, a sonic hedgehog mediator. Bone 29:54–61.

Kim HK, Feng GS, Chen D, King PD, Kamiya N. 2014. Targeted disruption of Shp2 in chondrocytes leads to metachondromatosis with multiple cartilaginous protrusions. J Bone Miner Res 29:761–769.

Kimura H, Ng JM, Curran T. 2008. Transient inhibition of the hedgehog pathway in young mice causes permanent defects in bone structure. Cancer Cell 13:249–260.

Koyama E, Leatherman JL, Noji S, Pacifici M. 1996. Early chick limb cartilaginous elements possess polarizing activity and express hedgehog-related morphogenetic factors. Dev Dyn 207:344–354.

Koyama E, Young B, Nagayama M, Shibukawa Y, Enomoto-Iwamoto M, Iwamoto M, Maeda Y, Lanske B, Song B, Serra R, Pacifici M. 2007. Conditional Kif3a ablation causes abnormal hedgehog signaling topography, growth plate dysfunction, and excessive bone and cartilage formation during mouse skeletogenesis. Development 134:2159–2169.

Koziel L, Kunath M, Kelly OG, Vortkamp A. 2004. Ext1-dependent heparan sulfate regulates the range of Ihh signaling during endochondral ossification. Dev Cell 6:801–813.

Kronenberg HM. 2003. Developmental regulation of the growth plate. Nature 423:332–336.

Kunkalla K, Liu Y, Qu C, Leventaki V, Agarwal NK, Singh RR, Vega F. 2013. Functional inhibition of BCL2 is needed to increase the susceptibility to apoptosis to SMO inhibitors in diffuse large B-cell lymphoma of germinal center subtype. Ann Hematol 92:777–787.

Lanske B, Karaplis AC, Lee K, Luz A, Vortkamp A, Pirro A, Karperien M, Defize LH, Ho C, Mulligan RC, Abou-Samra AB, Juppner H, Segre GV, Kronenberg HM. 1996. Pth/Pthrp receptor in early development and indian hedgehog-regulated bone growth. Science 273:663–666.

Lefebvre V, Bhattaram P. 2010. Vertebrate skeletogenesis. Curr Top Dev Biol 90:291–317.

Lefebvre V, de Crombrugghe B. 1998. Toward understanding Sox9 function in chondrocyte differentiation. Matrix Biol 16:529–540.

Lin AC, Seeto BL, Bartoszko JM, Khoury MA, Whetstone H, Ho L, Hsu C, Ali SA, Alman BA. 2009. Modulating hedgehog signaling can attenuate the severity of osteoarthritis. Nat Med 15:1421–1425.

Lin X. 2004. Functions of heparan sulfate proteoglycans in cell signaling during development. Development 131:6009–6021.

Lind T, Tufaro F, McCormick C, Lindahl U, Lidholt K. 1998. The putative tumor suppressors Ext1 and Ext2 are glycosyltransferases required for the biosynthesis of heparan sulfate. J Biol Chem 273:26265–26268.

Mackie EJ, Tatarczuch L, Mirams M. 2011. The skeleton: A multi-functional complex organ: The growth plate chondrocyte and endochondral ossification. J Endocrinol 211:109–121.

Minina E, Wenzel HM, Kreschel C, Karp S, Gaffield W, McMahon AP, Vortkamp A. 2001. BMP and IHH/PTHrP signaling interact to coordinate chondrocyte proliferation and differentiation. Development 128:4523–4534.

Mundlos S, Olsen BR. 1997. Heritable diseases of the skeleton. Part I: Molecular insights into skeletal development-transcription factors and signaling pathways. Faseb j 11:125–132.

Murtaugh LC, Chyung JH, Lassar AB. 1999. Sonic hedgehog promotes somitic chondrogenesis by altering the cellular response to BMP signaling. Genes Dev 13:225–237.

Park J, Zhang JJ, Moro A, Kushida M, Wegner M, Kim PC. 2010. Regulation of Sox9 by sonic hedgehog (Shh) is essential for patterning and formation of tracheal cartilage. Dev Dyn 239:514–526.

Pathi S, Rutenberg JB, Johnson RL, Vortkamp A. 1999. Interaction of IHH and BMP/Noggin signaling during cartilage differentiation. Dev Biol 209:239–253.

Porter DE, Simpson AH. 1999. The neoplastic pathogenesis of solitary and multiple osteochondromas. J Pathol 188:119–125.

Regard JB, Malhotra D, Gvozdenovic-Jeremic J, Josey M, Chen M, Weinstein LS, Lu J, Shore EM, Kaplan FS, Yang Y. 2013. Activation of hedgehog signaling by loss of Gnas causes heterotopic ossification. Nat Med 19:1505–1512.

Roberts DJ, Johnson RL, Burke AC, Nelson CE, Morgan BA, Tabin C. 1995. Sonic hedgehog is an endodermal signal inducing Bmp-4 and Hox genes during induction and regionalization of the chick hindgut. Development 121:3163–3174.

Romer JT, Kimura H, Magdaleno S, Sasai K, Fuller C, Baines H, Connelly M, Stewart CF, Gould S, Rubin LL, Curran T. 2004. Suppression of the Shh pathway using a small molecule inhibitor eliminates medulloblastoma in ptc1(+/−) p53(−/−) mice. Cancer Cell 6:229–240.

Scales SJ, de Sauvage FJ. 2009. Mechanisms of hedgehog pathway activation in cancer and implications for therapy. Trends Pharmacol Sci 30:303–312.
Seki K, Hata A. 2004. Indian hedgehog gene is a target of the bone morphogenetic protein signaling pathway. J Biol Chem 279:18544–18549.
St-Jacques B, Hammerschmidt M, McMahon AP. 1999. Indian hedgehog signaling regulates proliferation and differentiation of chondrocytes and is essential for bone formation. Genes Dev 13:2072–2086.
Stott NS, Chuong CM. 1997. Dual action of sonic hedgehog on chondrocyte hypertrophy: Retrovirus mediated ectopic sonic hedgehog expression in limb bud micromass culture induces novel cartilage nodules that are positive for alkaline phosphatase and type x collagen. J Cell Sci 110:2691–2701.
Vortkamp A, Lee K, Lanske B, Segre G V, Kronenberg HM, Tabin CJ. 1996. Regulation of rate of cartilage differentiation by Indian hedgehog and PTH-related protein. Science 273:613–622.
Wan M, Cao X. 2005. BMP signaling in skeletal development. Biochem Biophys Res Commun 328:651–657.
Williams JA, Guicherit OM, Zaharian BI, Xu Y, Chai L, Wichterle H, Kon C, Gatchalian C, Porter JA, Rubin LL, Wang FY. 2003. Identification of a small molecule inhibitor of the hedgehog signaling pathway: Effects on basal cell carcinoma-like lesions. Proc Natl Acad Sci USA 100:4616–4621.
Wu X, Cai ZD, Lou LM, Chen ZR. 2013. The effects of inhibiting hedgehog signaling pathways by using specific antagonist cyclopamine on the chondrogenic differentiation of mesenchymal stem cells. Int J Mol Sci 14:5966–5977.
Yauch RL, Gould SE, Scales SJ, Tang T, Tian H, Ahn CP, Marshall D, Fu L, Januario T, Kallop D, Nannini-Pepe M, Kotkow K, Marsters JC, Rubin LL, de Sauvage FJ. 2008. A paracrine requirement for hedgehog signalling in cancer. Nature 455:406–410.
Zou H, Wieser R, Massague J, Niswander L. 1997. Distinct roles of type I bone morphogenetic protein receptors in the formation and differentiation of cartilage. Genes Dev 11:2191–2203.

Supporting Information

Additional supporting information may be found in the online version of this article at the publisher's web-site